Anal. Chem. **2007,** *79,* 5614−5619

Apoferritin-Templated Synthesis of Encoded Metallic Phosphate Nanoparticle Tags

Guodong Liu, Hong Wu, Alice Dohnalkova, and Yuehe Lin*

Pacific Northwest National Laboratory, Richland, Washington 99352

Encoded metallic phosphate nanoparticle tags, with distinct encoding patterns, have been prepared using an apoferritin template. A center cavity structure as well as the dissociation and reconstructive characteristics of apoferritin at different pH environments provides a facile route for preparing such encoded nanoparticle tags. Encapsulation and diffusion approaches have been investigated during the preparation. The encapsulation approach, which is based on the dissociation and reconstruction of apoferritin at different pHs, exhibits an effective route to prepare such encoded metallic phosphate nanoparticle tags. The compositionally encoded nanoparticle tag leads to a high coding capacity with a large number of distinguishable voltammetric signals, reflecting the predetermined composition of the metal mixture solution (and hence the nanoparticle composition). Releasing the metal components from the nanoparticle tags at pH 4.6 acetate buffer avoids harsh dissolution conditions, such as strong acids. Such a synthesis of encoded nanoparticle tags, including single-component and compositionally encoded nanoparticle tags, is substantially simple, fast, and convenient compared to that of encoded metal nanowires and semiconductor nanoparticle (CdS, PbS, and ZnS) incorporated polystyrene beads. The encoded metallic phosphate nanoparticle tags thus show great promise for bioanalytical or product-tracking/identification/protection applications.

There has been considerable interest in recent years in synthesizing nanostructure materials across scientific and engineering disciplines because of their potential applications in bioassay, sensing, nanoscale electronic, mechanical, and magnetic devices.[1−5] Various nanomaterials, such as nanoparticles,[6−8] nanowires,[9,10] and nanotubes,[11−13] have been synthesized and used for different applications. Recently, the use of nanomaterials in the field of electroanalytical research has shown great promise because of its numerous signal amplifications and excellent electrocatalytic effects.[14,15] Metallic nanoparticles, such as gold,[16−18] silver,[19,20] indium,[21] and semiconductor nanoparticles (CdS, ZnS, and PbS),[22−24] have been widely used as tags for electrochemical biosensing, bioassays, and product identification. For example, Wang and co-workers reported on the use of CdS, ZnS, and PbS nanoparticles for electrochemical detection of proteins and DNA.[22,23] The prepared nanoparticles have also been incorporated into polystyrene beads with a predetermined ratio for product identification.[24] Keating and Natan also prepared metallic nanowires using a porous alumina membrane template for product identification.[25] Recently, Wang and Liu improved Keating's method and prepared compositionally encoded multimetal metal nanowire tags with distinct encoding patterns using a one-step templated electrodeposition from solutions containing different concentrations of various metal ions.[26] Synthesizing such metallic nanoparticles and nanowires requires a complicated and tedious process. Additionally, a harsh releasing step (namely, the dissolution of nanoparticle or nanowire tags with strong acid) is necessary before electrochemical detection. Herein, we present a simple and facile template-synthesis strategy based on the nanostructure protein, apoferritin, to prepare encoded metallic phosphate nanoparticle tags.

* Corresponding author. E-mail: yuehe.lin@pnl.gov. Phone: 01-509-3760529.

(1) (a) Penn, S. G.; He, L.; Natan, M. J. *Curr. Opin. Chem. Biol.* **2003**, *7*, 609−615. (b) Wang, J.; Liu, G.; Lin, Y. *Small* **2005**, *2*, 1134−1138. (c) Wang, J.; Liu, G.; Engelhard, M. H.; Lin, Y. *Anal. Chem.* **2006**, *78*, 6974−6979.
(2) (a) Rosi, N. L.; Mirkin, C. A. *Chem. Rev.* **2005**, *105*, 1547−1562. (b) Liu, G.; Lin, Y. *J. Nanosci. Nanotechnol.* **2005**, *5*, 1060−1065.
(3) Niemeyer, C. M. *Angew. Chem., Int. Ed.* **2001**, *40*, 4128−4158.
(4) (a) Lin, Y.; Lu, F.; Tu, Y.; Ren, Z. *Nano Lett.* **2004**, *4*, 191−195. (b) Lin, Y.; Yantasee, W.; Wang, J. *Front. Biosci.* **2005**, *10*, 492−505. (c) Liu, G.; Lin, Y. *Anal. Chem.* **2006**, *78*, 835−843.
(5) Xia, Y. N.; Yang, P. D.; Sun, Y. G.; Wu, Y. Y.; Mayers, B.; Gates, B.; Yin, Y. D.; Kim, F.; Yan, Y. Q. *Adv. Mater.* **2003**, *15* (5), 353−389.
(6) Taton, T. A.; Mirkin, C. A.; Letsinger, R. L. *Science* **2000**, *289*, 1757−1760.
(7) Bruchez, M.; Moronne, M.; Gin, P.; Weiss, S.; Alivisatos, A. P. *Science* **1998**, *281*, 2013−2016.
(8) Chan, W. C. W.; Nie, S. *Science* **1998**, *281*, 2016−2018.
(9) Cui, Y.; Wei, Q. Q.; Park, H. K.; Lieber, C. M. *Science* **2001**, *293*, 1289−1292.
(10) Law, M.; Goldberger, J.; Yang, P. D. *Ann. Rev. Mater. Res.* **2004**, *34*, 83−122.
(11) Iijima, S. *Nature* **1991**, *354*, 56−58.
(12) Nikolaev, P.; Bronikovski, M. J.; Bradley, K.; Rohmund, F.; Colbert, D. T.; Smith, K. A.; Smalley, R. E. *Chem. Phys. Lett.* **1999**, *313*, 91−97.
(13) Kohli, P.; Martin, C. R. *Nat. Rev. Drug Discovery* **2003**, *2*, 29−37.
(14) Wang, J. *Analyst* **2005**, *130*, 421−426.
(15) Wang, J. *Small* **2005**, *1*, 1036−1043.
(16) Dequaire, M.; Degrand, C.; Limoges, B. *Anal. Chem.* **2000**, *72*, 5521−5528.
(17) Gonzalez-Garcia, M. B.; Fernandez-Sanchez, C.; Costa-Garcia, A. *Biosens. Bioelectron.* **2000**, *15*, 315−321.
(18) Wang, J.; Xu, D.; Kawde, A.; Polsky, R. *Anal. Chem.* **2001**, *73*, 5576−5581.
(19) Wang, J.; Polsky, R.; Danke, X. *Langmuir* **2001**, *17*, 5739−5741.
(20) Cai, H.; Wang, Y.; He, P.; Fang, Y. *Anal. Chim. Acta* **2002**, *469*, 165−172.
(21) Wang, J.; Liu, G.; Jan, R.; Zhu, Q. *Anal. Chem.* **2003**, *75* (22), 6218−6222.
(22) Wang, J.; Liu, G.; Merkoçi, A. *J. Am. Chem. Soc.* **2003**, *125*, 3214−3215.
(23) Liu, G.; Wang, J.; Kim, J.; Jan, M.; Collins, G. *Anal. Chem.* **2004**, *76*, 7126−7130.
(24) (a) Wang, J.; Liu, G.; Rivas, G. *Anal. Chem.* **2003**, *75*, 4667−4671. (b) Wu, H.; Liu, G.; Wang, J.; Lin, Y. *Electrochem. Commun.* **2007**, *9*, 1573−1577.
(25) Keating, C. D.; Natan, M. J. *Adv. Mater.* **2003**, *15*, 451−454.
(26) Wang, J.; Liu, G. *Anal. Chem.* **2006**, *78*, 2461−2464.

10.1021/ac070086f CCC: $37.00
Published on Web 06/29/2007

Apoferritin is a native nanostructured protein composed of 24 polypeptide subunits that interact to form a hollow cagelike structure with a 12.5 nm diameter; the interior cavity of apoferritin is 8 nm in diameter and has an interior volume that can store up to 4500 iron atoms as an iron oxide−hydroxide mineral or hold 2000 iron atoms per apoferritin in iron phosphate form.[27] There are 14 channels connecting the outside of apoferritin with its interior, among which 6 are hydrophobic channels and 8 are hydrophilic channels. Because of its unique cavity structure characteristics, apoferritin has been used as a protein cage to synthesize size-restricted bioinorganic nanocomposites.[28−32] In this study, we used apoferritin as a template to prepare encoded nanoparticle tags with distinct voltammetric signatures, which could be used for electrochemical biosensing, bioassays, and product authenticity identification. Two approaches, diffusion and encapsulation, have been investigated. The characterization of the new compositionally encoded nanoparticles and their template-guided synthesis is reported in the following sections.

EXPERIMENTAL SECTION

Apparatus. Electrochemical measurements were performed with an electrochemical analyzer CHI 660A (CH Instruments, Austin, TX) connected to a personal computer. Transmission electron microscopy (TEM) imaging and high-resolution TEM analysis were carried out on a Jeol JEM 2010 microscope with a specified point-to-point resolution of 0.194 nm. The operating voltage on the microscope was 200 keV. For negative stain, NanoW (Nanoprobes) solution was applied on a grids with material suspension. All images were digitally recorded with a slow-scan charged-coupled device camera (image size 1024 × 1024 pixels), and image processing was carried out using a digital micrograph (Gatan). A PD-10 column (GE Health) packed with Sephadex G-25 was used to purify apoferritin. Inductively coupled plasma (ICP) analysis was performed with an Optima 3000 DV ICP-AES (Perkin-Elmer).

Reagents. All stock solutions were prepared with deionized water. Tris−HCl buffer (0.1 M, pH = 8.0) was made from 1 M stock buffer, which was purchased from Sigma. Lead nitrate, cadmium chloride, and zinc nitrate were purchased from Aldrich. Apoferritin was purchased from Sigma. The solution of mercury atomic absorption standard (1010 mg/L) was purchased from Aldrich.

Preparation of Metallic Phosphate Nanoparticles. *Encapsulation Approach.* Apoferritin with a concentration of 25 mg/mL was first diluted with 0.01 M phosphate buffer saline (PBS) to make a 2.5 mL solution. The diluted apoferritin was loaded on a PD-10 column and was washed with 4 mL of 0.01 M PBS. An aliquot of 2 mL of the purified apoferritin was transferred into an 8 mL cell. The solution pH was first adjusted to 2 with 1 M HCl while magnetically stirring the mixture. Approximately 250 μL of 10 mM cadmium chloride (or lead nitrate, zinc nitrate, respectively, or a mixture in a different ratio) was slowly added into the apoferritin solution at this pH condition. Then the pH was adjusted to 8.5 with 0.1 M NaOH added dropwise. The mixture was continuously stirred for 2 h to allow the metal to form a phosphate metal core inside apoferritin. The mixture was subjected to centrifugation at 7826*g* for 5 min. The supernatant was washed three times with 0.1 M Tris−HCl using an Amicon filter (MWCO = 25 000). Then, the encoded metallic phosphate/apoferritin nanoparticles were reconstituted into a 0.5 mL solution. The protein concentration was determined using a bicinchoninic acid (BCA) assay with bovine serum albumin as the standard. Metals entrapped in the apoferritin nanoparticles were analyzed with ICP-AES by diluting the reconstituted nanoparticle solution 100 times in 2% nitric acid.

Diffusion Approach. Approximately 500 μL of 10 mM cadmium nitrate (or lead nitrate) was slowly added into the purified apoferritin solution (prepared in 0.1 M Tris buffer, pH = 8.0, 3 mL), and the mixture was continuously stirred for 1 h to allow the cadmium ions to diffuse into the cavity of apoferritin. Subsequently, 500 μL of 0.2 M phosphate buffer (pH = 7.0) was slowly introduced (drop-by-drop) into the solution to form a phosphate metal core inside the apoferritin. Excess metal cations remaining outside the apoferritin were precipitated with phosphate buffer. After 30 min, the mixture was subjected to centrifugation at 7826*g* for 5 min. The supernatant was washed three times with 0.1 M Tris−HCl using an Amicon filter (MWCO = 25 000). Then, the encoded metallic phosphate apoferritin nanoparticles were reconstituted into a 1 mL solution. The protein concentration was determined using a BCA assay with bovine serum albumin as the standard. Control experiments were performed under the same conditions in the absence of apoferritin.

Electrochemical Detection. Square-wave voltammetric (SWV) measurements were performed with an in situ plated mercury film glassy carbon electrode as the working electrode and Ag/AgCl and platinum wire as the reference electrode and counter electrode, respectively. A 0.2 M acetate buffer (pH = 4.6) containing 10 μg mL^{-1} was used as the supporting electrolyte. Before electrochemical detection, single-component or compositionally encoded metallic phosphate nanoparticle tags (5 μL) were added to the acetate buffer (2 mL, pH 4.6), and the solution was stirred 1 min to release the metal ions from the metallic phosphate. The released metal ions were measured with SWV (in a stirred acetate buffer solution) using an in situ plated mercury film on a glassy carbon electrode, following a 1 min pretreatment at 0.6 V and using a 1.5 min accumulation at −1.4 V. Subsequent square-wave stripping was performed after a 15 s rest period (without stirring) from −1.4 to −0.4 V with a step potential of 4 mV, an amplitude of 20 mV, and a frequency of 25 Hz. A baseline correction of the resulting voltammogram was performed using CHI 660A software.

RESULTS AND DISCUSSION

In this study, apoferritin was used as the template for preparing encoded metallic phosphate nanoparticle tags. Because of the characteristics of the specific structure (center cavity and multichannel) of apoferritin as well as its dissociation and reconstruction at different pHs, two approaches were employed during the preparation of nanoparticle tags. Figure 1 schematically illustrates

(27) Ford, G. C.; Harrison, P. M.; Rice, D. W.; Smith, J. M. A.; Treffry, A.; White, Y. J. *Philos. Trans. R. Soc. London, Ser. B* **1984**, *304*, 551−565.
(28) Meldrum, F. C.; Wade, V. J.; Nimmo, D. L.; Heywood, B. R.; Mann, S. *Nature* **1991**, *349*, 684−686.
(29) Douglas, T.; Dickson, D. P. E.; Betteridge, S.; Charnock, J.; Garner, C. D.; Mann, S. *Science* **1995**, *269*, 54−57.
(30) Meldrum, F. C.; Heywood, B. R.; Mann, S. *Science* **1992**, *257*, 522−523.
(31) DomQnguez-Vera, J. M.; Colacio, E. *Inorg. Chem.* **2003**, *42*, 6983−6985.
(32) Galvez, N.; Sanchez, P.; DomQnguez-Vera, J. *Dalton Trans.* **2005**, 2492−2494.

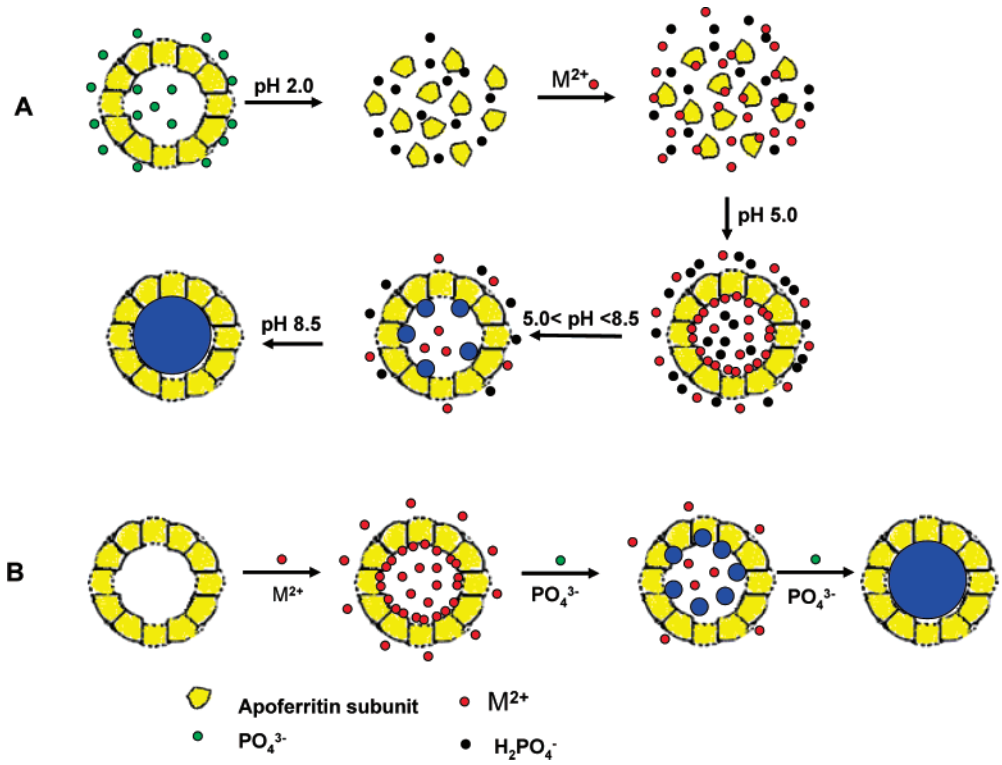

Figure 1. Schematic illustration of apoferritin-templated synthesis of encoded metallic phosphate nanoparticle tags: (A) encapsulation; (B) diffusion.

the procedures. The first approach, namely, encapsulation (Figure 1A), is proceeded by adjusting the pH of the apoferritin solution to encapsulate metal phosphate in the cavity of apoferritin. Briefly, the apoferritin prepared in phosphate buffer (0.01 M) is dissociated into its subunits at pH 2. This pH is maintained for 20 min. Metal ions are slowly introduced into the solution. At this pH, phosphate ions react with the hydrogen ion to form dihydrogen phosphate cations and coexist with metal ions and will not form the metal phosphate precipitates. Because the inner surface of the apoferritin cavity has many amino acid residues, the inner space has a negative electrostatic potential.[33] The metal ions will be concentrated in the inner surface of apoferritin subunits. With the increase of the pH (5.0), the subunits start to reconstitute to form the cavity structure; thereby, both metal cations and phosphate anions are trapped inside the protein cage simultaneously. The metal ions will be concentrated inside the apoferritin cavity. With the increase of the pH (>5), dihydrogen phosphate anions become phosphate ions and start to precipitate with metal ions to form metal phosphate seeds at the inner surface of the apoferritin cavity. Once the metal phosphate seeds have formed, the metal phosphate crystal surface itself will work as an autocatalyst and the precipitation reaction will continue to fill up the apoferritin cavity. Metal ions and phosphate cations outside apoferritin will diffuse into the cavity of apoferritin because of the concentration difference between inside and outside apoferritin. The process will be maintained for 2 h at pH 8.5. At this point, the reconstituted apoferritin is further aged to form the stable cage structure and the metal phosphate core will be formed in the cavity of apoferritin. It is noted that slowly adjusting the pH to 5 is critically important in reconstructing highly loaded apoferritin nanoparticles.

The second approach, namely, diffusion (Figure 1B), includes two diffusing steps. Metal ions first diffuse into the apoferritin cage through channels at a pH of 8 and accumulate on the internal surface through the interaction between metal ions and the functional groups on internal surface. After a 1 h balance, phosphate buffer is slowly introduced into the solution. Because the concentration of metal ions in the surface of the cavity is higher than that outside of the cavity, precipitation will first occur inside apoferritin to form metal phosphate seeds in the inner surface of the cavity. Once the metal phosphate seeds have formed in the cavity of the apoferritin, the concentrations of metal ions and phosphate in the cavity will decrease, the metal ions and phosphate cations outside the apoferritin will diffuse into the cavity. The metal phosphate seed itself will work as an autocatalyst, and metal phosphate will be formed quickly in the apoferritin cavity. This process will take 30 min to complete. The mechanism of apoferritin-templated metal nanoparticles formation by the diffusion process has been described previously.[33]

Initial studies were started to prepare single-component metal phosphate nanoparticles. A cadmium phosphate nanoparticle tag was prepared first with the above procedures. To confirm the formation of cadmium phosphate nanoparticles, TEM was use to study the sizes and distributions of nanoparticles. Figure 2A presents the TEM image of an unstained cadmium phosphate sample, which was prepared by the encapsulation method. One can see that individual particles are clearly identifiable and the dense cadmium phosphate cores appear black and are surrounded by an amorphous shell in this unstained sample. The selected area electron diffraction image (Figure 2B) gave powder ring patterns indicating the formed cadmium phosphate was crystalline. To observe the core−shell structure clearly, negatively stained sample was prepared for TEM (Figure 2C). It can be seen that

(33) Iwahori, K.; Yoshizawa, K.; Muraoka, M.; Yamashita, I. *Inorg. Chem.* **2005**, *44*, 6393−6400.

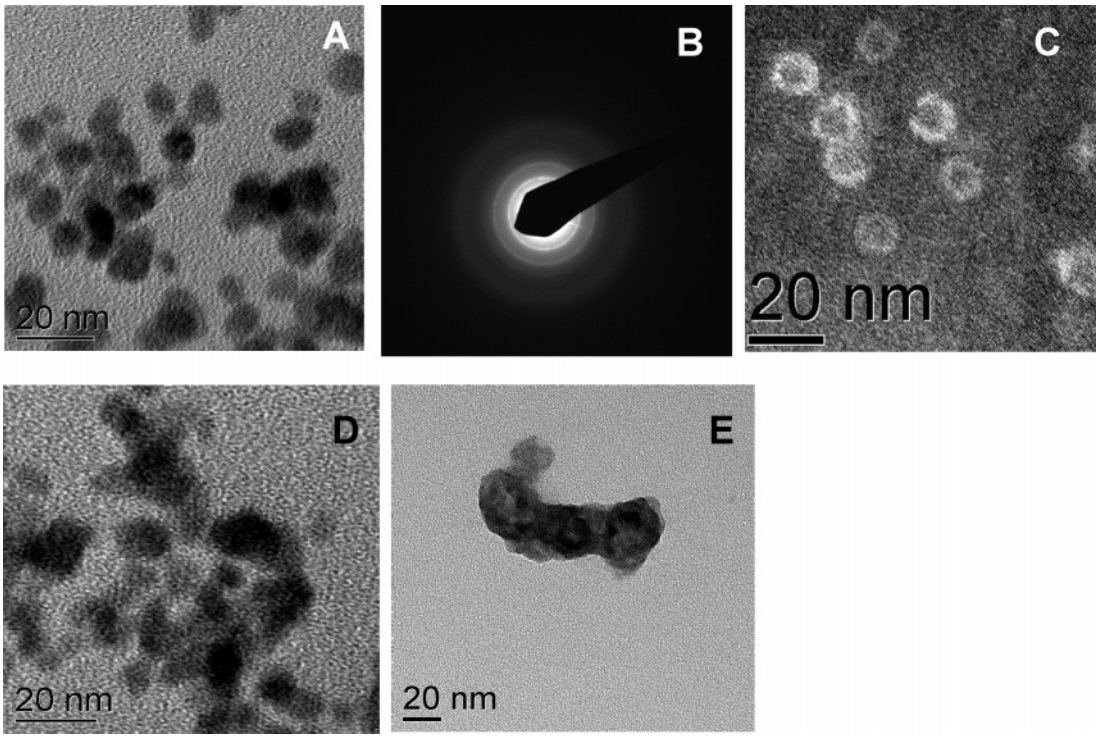

Figure 2. (A) Typical TEM image of an unstained sample of cadmium phosphate nanoparticles based on the encapsulation approach. (B) Corresponding electron diffraction pattern of (A). (C) Typical TEM image of a stained sample of cadmium phosphate nanoparticles based on the encapsulation approach. (D) Typical TEM image of an unstained sample of cadmium phosphate nanoparticles based on the diffusion approach. (E) TEM image of an unstained control sample. The control sample was prepared under the same conditions in the absence of the apoferritin template.

the cadmium phosphate core (black) with a diameter of around 8 nm was surrounded with a protein shell (white). This indicates that the protein shell of the apoferritin remained a substantially stable structure and sustained no major alteration during the dissociation and reconstruction process. This is consistent with our previous observation (hexacyanoferrate- and fluorescein-loaded apoferritin tags).[34] Figure 2D is the TEM image of an unstained cadmium phosphate nanoparticle sample prepared with the diffusion method (approach B). One can see that the particle size distribution is not uniform. It may be caused by the aggregations of apoferritin during the diffusion process of the metal ions. Similar phenomena were also observed with other metal phosphates (results not shown). A control experiment was also performed under the same conditions in the absence of the apoferritin template. TEM analysis (Figure 2E) revealed that cadmium phosphate clusters were formed during the preparation and no discrete nanoparticle was observed.

Compositionally encoded metal phosphate nanoparticle tags were also prepared by the encapsulation and diffusion methods with mixed metal ions, which have predetermined ratios. The loading amount of metal ions per apoferritin was estimated by comparing the concentrations of apoferritin and metal ions in the nanoparticle solution. The apoferritin concentration was determined by the BCA method. The concentration of metal ion was determined by ICP. Table 1 summarizes the measurement results of the prepared nanoparticle tags with the two methods. The ratios of metals show good agreement with the predetermined amount for compositionally encoded nanoparticle tags prepared with the encapsulation method. However, there is no agreement between the ratios of metal and the predetermined amount for the compositionally encoded nanoparticle tags prepared with the diffusion method. It appears from the data that the cadmium ions appear to be incorporated much more effectively than lead in the case of the diffusion method. The result is consistent with a previous report, which stated that cadmium had the highest stoichiometric binding to the inner cavity wall of the polypeptide shell of apoferritin.[35] The reason may come from the different diffusion capabilities of metal ions and phosphate anions in the apoferritin channel. Since the nature of the apoferritin channels is unclear, Okuda et al.[36] assumed that only cations can pass through the channels. Massover[37] proposed a dynamic dissociation of apoferritin subunits, enabling the entry of larger molecules and anions into the apoferritin cavity. Therefore, the encapsulation approach was used to prepare the compositionally encoded nanoparticle tags for further applications.

The concentration of metal ions during encapsulation was optimized to achieve the highest loading capacity. It was found that a high concentration of metal ions (>10 mM) caused the heavy aggregation of apoferritin, leading to a significant decrease of protein concentration. An approximately 10 mM metal ion in

(34) (a) Liu, G.; Wang, J.; Wu, H.; Lin, Y. *Anal. Chem.* **2006**, *78*, 7471. (b) Liu, G.; Wang, J.; Lin, Y. *ChemBioChem* **2006**, *7* (9), 1315−1319.

(35) Wong, K. K. W.; Mann, S. *Adv. Mater.* **1996**, *8*, 928−932.

(36) Okuda, M.; Iwahori, K.; Yamashita, I.; Yoshimura, H. *Biotechnol. Bioeng.* **2003**, *84* (2), 187−194.

(37) Massover, W. H. Dynamic stability of apoferritin a new model to explain how impermeable reagents can reduce/capture iron within ferritin. In *Iron Biomaterials*; Frankel, R. B., Blakemore, R. P., Eds.; Plenum Press: New York.

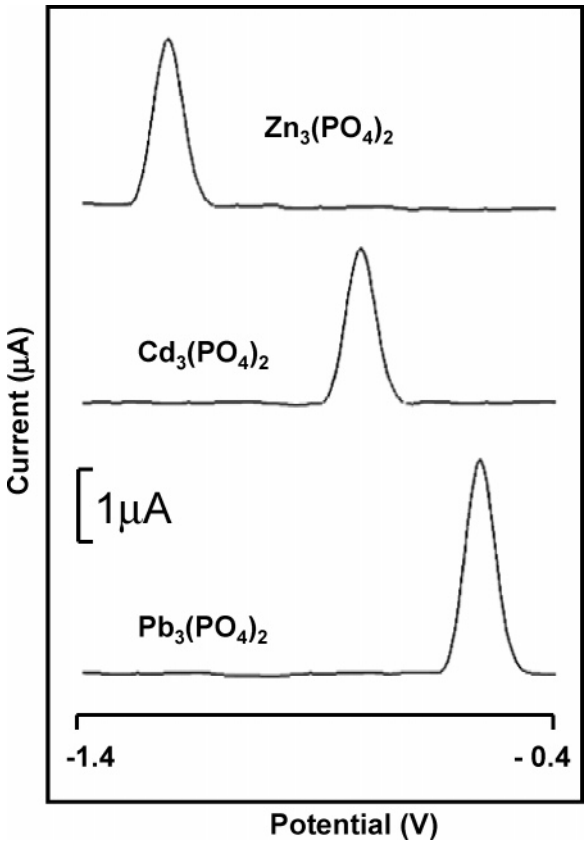

Figure 3. Typical SWVs of single-component metal phosphate nanoparticles in 0.2 M acetate buffer (pH 4.6) containing 10 μg mL^{-1} mercury. Voltammetric stripping readout with an in situ plated mercury-coated glassy carbon electrode, using a 1 min pretreatment at 0.6 V, a 1.5 min accumulation at −1.4 V, a 15 s rest period (without stirring), an SWV scan with a step potential of 50 mV, an amplitude of 20 mV, and a frequency of 25 Hz. Background correction was accomplished using CHI 660A software.

Table 1. Summary of the Calculation Results of Compositionally Encoded Metallic Phosphate Nanoparticles

method	compositionally encoded nanoparticle (Cd/Pb ± SD)[a]
encapsulation	1.00/1.05 ± 0.02 (added 1/1)
	1.00/1.94 ± 0.01 (added 1/2)
diffusion	2.10/1 ± 0.01 (added 1/1)
	1.00/1.30 ± 0.03 (added 1/2)

[a] SD: standard deviation, $n = 6$.

the encapsulation solution resulted in the maximum loading of metal per apoferritin (results not shown). We calculated the loading amount of metal ions per apoferritin by comparing the concentrations of apoferritin and metal ions in the nanoparticle solution. The concentrations of apoferritin and metal ions were determined by the BCA method and ICP, respectively. For single-component cadmium phosphate nanoparticles, the numbers of metal ions are 1340 per apoferritin with a standard deviation of ±80 ($n = 6$).

Voltammetric signatures of the encoded metallic phosphate nanoparticle tags were tested by SWV. Figure 3 displays typical voltammograms of single-component metallic phosphate nanoparticle tags (cadmium phosphate, lead phosphate, and zinc

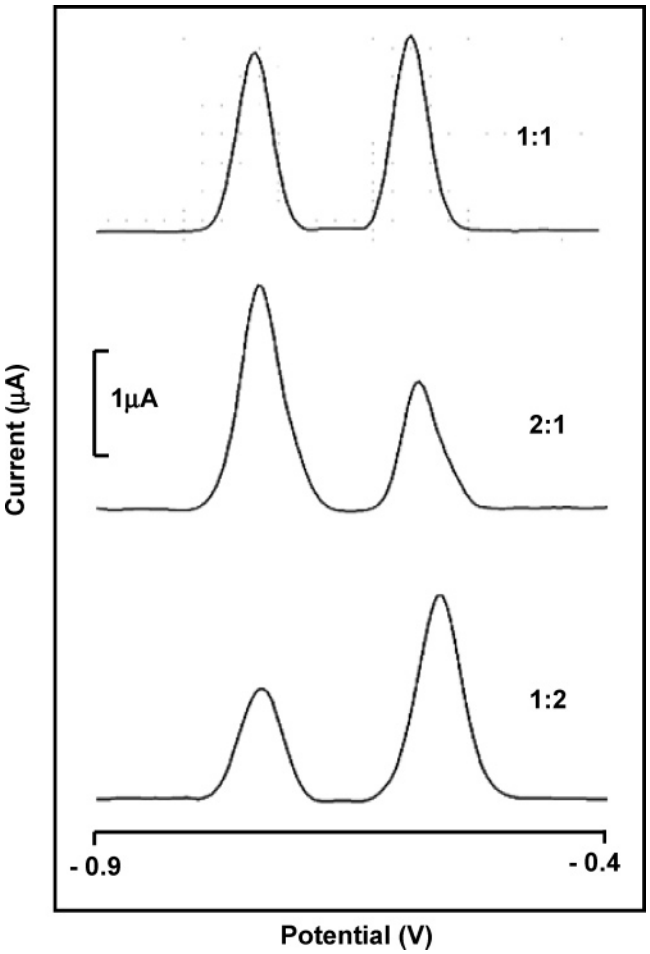

Figure 4. Typical stripping voltammograms for compositionally encoded metallic phosphate nanoparticles with a predetermined metal ratio: (top) Cd/Pb 1:1, (middle) Cd/Pb 2:1, and (bottom) Cd/Pb 1:2. Other conditions are as in Figure 3.

phosphate) prepared with encapsulation methods. The SWV measurements were performed with a cleaned glassy carbon electrode in 0.2 M acetate buffer (pH 4.6) containing 10 μg mL^{-1} mercury. The acetate buffer with pH 4.6 would dissolve metal phosphate nanoparticles to obtain free metal ions. We can see that each nanoparticle yields a characteristic voltammogram with a well-defined peak at −1.20 (zinc phosphate), −0.78 (cadmium phosphate), and −0.55 V (lead phosphate). The voltammetric behaviors of such metallic phosphate nanoparticles are similar to that of metal sulfide semiconductor nanoparticles (ZnS, CdS, and PbS).[22,23] The promising voltammetric signatures of metallic nanoparticles thus open a new door to prepare such nanoparticle tags for biosensor, bioassay, and product identifications.

For encoded nanoparticle tags, compositionally encoded nanoparticles would have numerous advantages compared to single-component encoded nanoparticles because they will provide a large variability of distinct voltammetric codes. ICP experiments initially showed that the encapsulation method with an apoferritin template would easily prepare compositionally encoded nanoparticle tags, which reflected the predetermined composition of the metal ion mixture solution. Such use of compositionally encoded nanoparticle tags to generate distinct voltammetric bar code patterns is illustrated below with two-metal (Cd and Pb) encoded nanoparticles. Figure 4 displays typical voltammograms of com-

positionally encoded nanoparticles prepared from solutions containing different concentration ratios of their cadmium and lead constituents [1:1 (top), 2:1 (middle), and 1:2 (bottom)]. Each nanoparticle yields a characteristic multipeak voltammogram with sharp, symmetric, and baseline-resolved peaks. The different nanoparticle compositions have no effect upon the peak separation. There is slight shift of lead peak potentials with the different nanoparticle compositions. This slight shift is not large enough to cause confusion as to the identity of the peak. The ratios of current intensities correlate well with the predetermined concentration of the metal in the prepared solution. Apparently, and as expected, the composition of the compositionally encoded nanoparticles and hence the resulting bar code patterns are controlled by the composition of the prepared solution. In comparison with the preparation of encoded metallic nanowires, which are based on the porous alumina membrane template and electrochemical deposition,[26] the apoferritin template-based route provides a simple and convenient route to prepare such encoded nanocomposite. Because electrochemical detection can measure five to six metals simultaneously in a single run (with minimal peak overlap),[38,39] it is possible to achieve thousands of usable voltammetric signatures with four or five metal components present at five or six concentration ratios.

It is very important to obtain reproducible results using such an encoded nanoparticle tag, particularly in the product authenticity test. A highly reproducible detection will avoid false positive and negative results. The precision and uniformity of the apoferritin template-directed synthesis of the compositionally encoded nanoparticle tags were examined by plotting a histogram for each current intensity in connection with six different suspensions of nanoparticles (Figure 5). We can see that the electrochemical signals (current) are highly reproducible with a relative standard deviation of 2.3% and 4.2% for Cd and Pb, respectively. The ratio of the mean peak currents follows closely their original concentration ratio in the preparation solution (2:1).

In conclusion, we have demonstrated that apoferritin could be used as a template to prepare single-component and compositionally encoded metallic nanoparticle tags with distinct and recognizable voltammetric signatures. Encapsulation and diffusion approaches have been investigated during the preparations, and the encapsulation approach enables the successful control of the multiple metal composition ratios in compositionally encoded nanoparticles. The new templated synthesis of metallic phosphate nanoparticles is substantially simpler and faster than preparing multisegment and compositionally encoded metal nanowires by electrodepositing metal ions in a porous alumina membrane template. Releasing the metal components from metallic phosphate nanoparticles in the electrochemical detection buffer avoids a harsh dissolution step (for example, strong acid to dissolve metal nanowires or metal sulfide nanoparticles). The resulting electrochemical signatures from the compositionally encoded nanoparticle tags correlate well with the predetermined concentration ratio and indicate a reproducible encapsulation process. The new encoded metallic phosphate nanoparticle tags thus represent a useful addition to the arsenal of particle-based product-tracking/identification/protection. The encoded nanoparticles also offer great promise for multiplex electrochemical biosensors and bioassays.

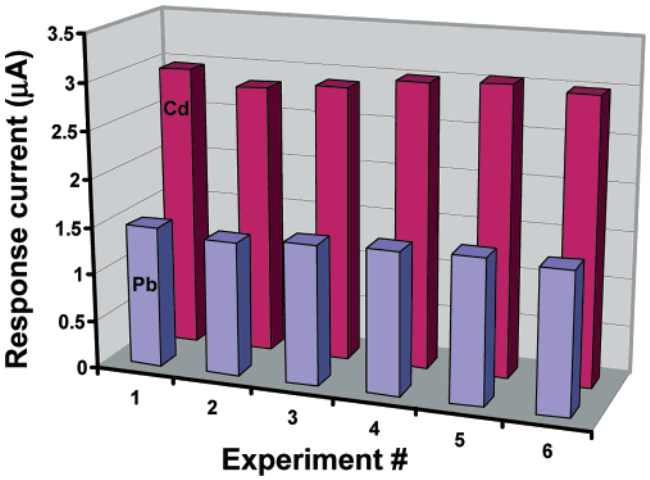

Figure 5. Reproducibility of the compositionally encoded nanoparticle voltammetric signatures using six different nanoparticle suspensions and a predetermined concentration ratio in the preparation solution of 2.0 Cd/1.0 Pb. Other conditions are as in Figure 3.

ACKNOWLEDGMENT

This work was partially supported by Grant 1 U01 NS058161-01 from the National Institute of Neurological Disorders and Stroke (NINDS), NIH and partially by CDC/NIOSH Grant R01 OH008173-01. The research described in this paper was performed at the Environmental Molecular Sciences Laboratory, a national scientific user facility sponsored by DOE's Office of Biological and Environmental Research and located at Pacific Northwest National Laboratory, which is operated by Battelle for DOE under Contract DE-AC05-76RL01830.

Received for review January 14, 2007. Accepted May 22, 2007.

AC070086F

(38) Wang, J. *Stripping Analysis*; VCH Publishers: Deerfield Beach, FL, 1985.
(39) Jagner, D. *Trends Anal. Chem.* **1983**, *2*, 53−56.